10-1-2020

Hydrologic impacts and trade-offs associated with developing oil palm for bioenergy in Tabasco, Mexico

Azad Heidari
Michigan Technological University

Alex Mayer
Michigan Technological University, asmayer@mtu.edu

David Watkins
Michigan Technological University, dwatkins@mtu.edu

María Mercedes Castillo
El Colegio de la Frontera Sur

Journal of Hydrology: Regional Studies 31 (2020) 100722

Contents lists available at ScienceDirect

Journal of Hydrology: Regional Studies

journal homepage: www.elsevier.com/locate/ejrh

Hydrologic impacts and trade-offs associated with developing oil palm for bioenergy in Tabasco, Mexico

Azad Heidari[a], Alex Mayer[a,*], David Watkins Jr.[a], María Mercedes Castillo[b]

[a] Department of Civil and Environmental Engineering, Michigan Technological University, Houghton, MI, USA
[b] Departamento de Ciencias de la Sustentabilidad, El Colegio de la Frontera Sur, Villahermosa, Tabasco, Mexico

ARTICLE INFO

Keywords:
Land use change
Hydrologic modification
Oil palm development
Bioenergy
Watershed hydrology modeling

ABSTRACT

Study region: Oil palm cultivation has rapidly expanded worldwide due to demands for food oils and the potential for liquid fuel production. However, there is a scarcity of research on the hydrologic impacts of oil palm plantations at a watershed scale, especially in Latin America. We focus on a watershed typical of intensive palm oil production in Tabasco, Mexico.

Study focus: A Soil and Water Assessment Tool model was calibrated to simulate long-term streamflow in the study watershed. The plant growth module was calibrated for leaf area index (LAI) and fruit yield simulations. Oil palm development scenarios were simulated to investigate the impacts of planting density and converted land cover types.

New hydrological insights for the region: Oil palm evapotranspiration rates were 51 % higher on average than the converted land covers. The higher water use reduced mean annual streamflow by only 9% at the watershed scale, due to high precipitation in the upper watershed. In contrast, a 15 % decline in annual water yield was simulated in the converted areas of the watershed. Corresponding streamflow reductions in low-flow months were on average 34 %. A planting density of 150 palm/ha was the most efficient for water use and fruit production, giving a green water footprint for producing biodiesel of 87 m^3/GJ energy, similar to oil palm cultivation elsewhere in the world.

1. Introduction

The African oil palm (*Elaeis guineensis*) can produce 4 – 5 ton/ha of oil, which is among the highest yields for the oil crops (Corley and Tinker, 2008; Mukherjee and Sovacool, 2014). Palm oil is used for biofuels in addition to cooking oil and as an ingredient in personal care products and processed foods (Mukherjee and Sovacool, 2014). Oil palm is the fastest expanding tree species in humid tropical low lands, especially in Southeast Asia (FAOSTAT, 2017). Land area for oil palm cultivation increased from 10 to 17 million ha from 2000 to 2012 (Pirker et al., 2016), resulting in attention to the environmental impacts of conversion to palm oil. Most of the research on environmental impacts of oil palm conversion has focused on deforestation and consequent greenhouse gas impacts and loss of biodiversity (Pirker et al., 2016; Vijay et al., 2016). The impacts of oil palm on hydrologic cycling are less well publicized or understood (Comte et al., 2012; Larsen et al., 2014; Carlson et al., 2014; Meijide et al., 2018; Manoli et al., 2018). Oil palm requires humid, warm conditions, such as those found in the tropics, to produce high yields (Sheil et al., 2009). While the tropics are renowned as water-rich, oil palm yields could be increased substantially by irrigation in regions with greater variability or lower rainfall (Ludwig et al., 2011; Dislich et al., 2017; Woittiez et al., 2017). Land drainage for oil palm cultivation can result in soil

* Corresponding author. Present address: Department of Civil Engineering, University of Texas at El Paso, El Paso, TX, USA.
E-mail address: asmayer2@utep.edu (A. Mayer).

https://doi.org/10.1016/j.ejrh.2020.100722
Received 11 February 2020; Received in revised form 9 June 2020; Accepted 5 August 2020
Available online 01 September 2020

subsidence and associated increases in flood risk (Sumarga et al., 2016). Furthermore, conversion of tropical forests to oil palm can decrease streamflows substantially during dry seasons or droughts (Bruijnzeel, 2004; Yusop et al., 2007; Adnan and Atkinson, 2011; Merten et al., 2016; Dislich et al., 2017; Tarigan et al., 2020). Research on the impacts of oil palm cultivation on hydrology has focused primarily on plot-scale studies of ecohydrologic fluxes, such as the impact of tree age on canopy rainfall interception (Farmanta and Dedi, 2015; Chong et al., 2018) and transpiration rates in palms with varying ages and grown on different slopes (Röll et al., 2015; Hardanto et al., 2017). A small number of modeling studies have been used to investigate impacts from oil palm conversion, focusing on nutrient cycling (Babel et al., 2011) at the watershed scale and carbon-water-energy budgets at the plot scale (Manoli et al., 2018).

The tradeoffs between oil palm production and hydrologic impacts have been acknowledged, but there are no studies of how management of oil palm cultivation could mitigate these tradeoffs at the plantation and watershed scales. Ultimately, optimizing water use and oil palm production could result in more efficient land use and reduce conversion from natural landscapes. Moreover, while most of the studies on impacts of oil palm cultivation on hydrology have focused on Southeast Asia, there is little published on these impacts in tropical Latin America regions experiencing oil palm expansion (Gilroy et al., 2015; Furumo and Aide, 2017). While deforestation due to oil palm cultivation occurs in Latin America (Vijay et al., 2016), as in Southeast Asia, the primary mode of conversion in Latin America is the transformation of cattle pasture to oil palm (Furumo and Aide, 2017; Ramankutty and Graesser, 2017). Thus, there is little information on how land use change from existing land use to oil palm cultivation impacts, or will impact, hydrologic cycling in the tropical Latin America setting. Our study area is located in the Mexican states of Tabasco and Chiapas, which underwent rapid deforestation to pasture lands in the late 1900s and is now experiencing oil palm conversion at a rapid rate. In Mexico at large, oil palm-cultivated area increased 485 % from 2003 to 2017 (FAOSTAT, 2017).

The goal of this study is to determine how oil palm cultivation practices impact hydrologic cycling, including evapotranspiration (ET), streamflows, and water yields, at local and watershed scales in a Latin American setting. A calibrated Soil Water Assessment Tool (SWAT) (Arnold et al., 2012) hydrologic-agronomic model is used to simulate hydrologic fluxes and oil palm fruit production. The simulation results are synthesized to assess tradeoffs between hydrologic impact, e.g. streamflows and water yields, and bioenergy feedstock production, e.g. oil palm production, for a range of management scenarios. Management scenarios based on the land use classes to be converted from present use to oil palm, oil palm planting densities, and maximum land slopes are formulated and simulated to investigate how tradeoffs between oil palm fruit production and streamflow change with spatial scale and alternative management practices

2. Materials and methods

2.1. Study site, calibration and validation

The study watershed, which includes areas in Tabasco and Chiapas, Mexico (Fig. 1), was selected based on data availability and proximity to existing oil palm plantations in the region. The watershed land use is predominantly pasture for cattle raising, crop production, and forests. The majority of the remaining forest is found at higher elevations and slopes. Long-term daily flow records from the Pichucalco hydrologic station (http://www.conagua.gob.mx) were used for hydrologic calibration and validation purposes. The contributing area to the gauge was estimated as 361 km^2, based on 15-meter resolution digital elevation model provided by the National Institute of Statistics and Geography (Instituto Nacional de Estadística y Geografía- INEGI, 2020). The simulated watershed was extended 22 km downstream of the Pichucalco hydrologic station to capture more low-slope areas typical of oil palm plantations in the study region, resulting in a watershed area of 561 km^2. A customized streamline shapefile from CONAGUA (http://www.conagua.gob.mx/) was used for stream delineation. Land use-land cover (LULC) maps for 2000 and 2014 and soil maps were obtained from INEGI.

Maximum and minimum daily temperature and daily precipitation were compiled from the National Climatological database (Base de datos climatológica nacional, http://clicom-mex.cicese.mx). In addition, Climate Forecast System Reanalysis (CFSR) global weather data (https://globalweather.tamu.edu) was added to the SWAT weather database (Fuka et al., 2014). Spatial interpolation of the climate data indicates that the area receives an average of almost four meters (3960 mm) of precipitation annually, with the majority of rainfall occurring during June to October (see Fig. 2). Precipitation is higher in the southern portion of the watershed (see Fig. 1), where elevation increases to 2100 m ASL. The average annual temperature in the watershed is 25.2 °C, with slight variation across the watershed. Fig. 2 shows the intra-annual variation of streamflow, temperature, and precipitation. The highest monthly average streamflow is in October, as a result of heavy rain events, with the lowest flow months occurring in March through May. Streamflows are higher than precipitation in the cool-weather months (October through March) because baseflows contribute to a greater amount of streamflow during those months (116 mm/yr on average in the cool weather months vs. 80 mm/yr in the remaining months).

Hydrologic and vegetation growth models were set up in SWAT to allow the investigation of oil palm planting density and the impacts of land conversion policies. ArcSWAT version 2012.10_4.19 (Winchell et al., 2013) was used to incorporate the year 2000 land use-land cover (LULC) map for the region, which most closely aligns with the historical streamflow data. The watershed was divided into 9 sub-watersheds and 142 non-contiguous hydrologic response units (HRUs), which represent homogeneous areas within each sub-basin with unique combinations of land use, soil type and slope class. Thresholds of 0%, 10 % and 10 % were selected for LULC, soils, and slope classes, respectively, for the HRU definition.

Calibration and validation focused on both the hydrological and plant growth components of the model. The hydrologic calibration and validation was performed with 22 years (from 1962 to 1983) of daily streamflow to include a combination of dry and wet

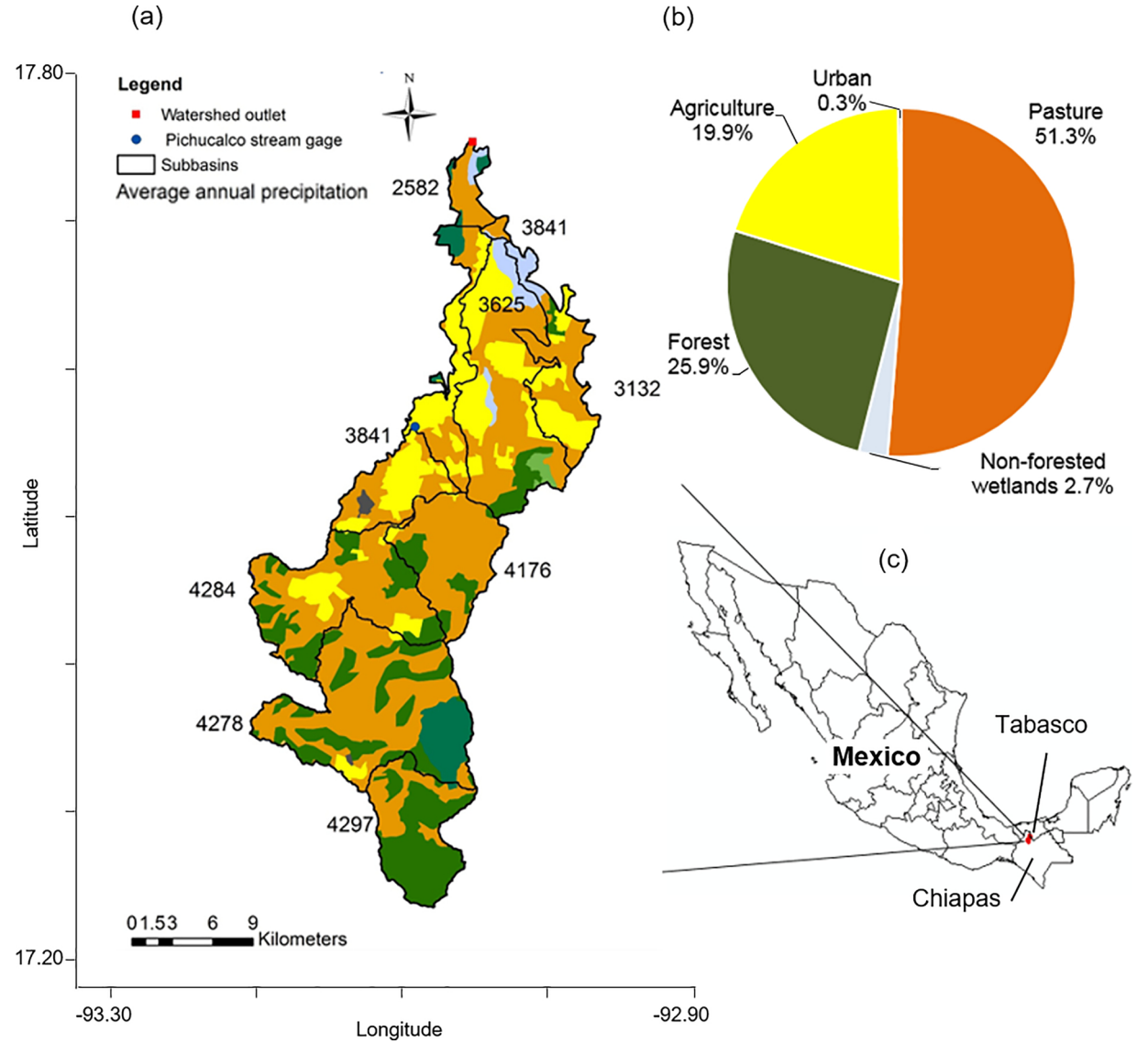

Fig. 1. (a) Land use-land cover map of the Pichucalco River watershed, location of streamflow gauge and watershed outlet, sub-basin boundaries, and average annual precipitation (in mm) for each sub-basin; (b) overall land use-land cover fractions for the Base Case scenario; and (c) study site location in the states of Tabasco and Chiapas, Mexico.

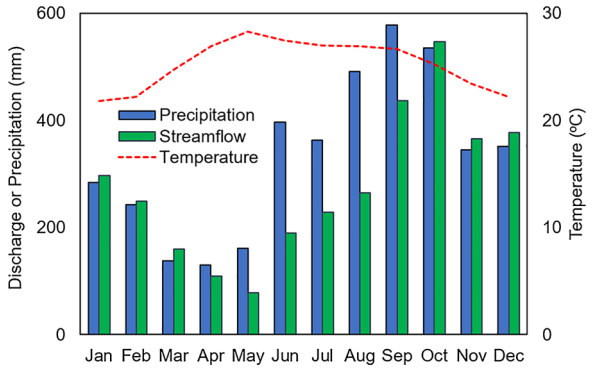

Fig. 2. Intra-annual patterns of average precipitation, streamflow normalized by watershed area, and temperature in the watershed (mean values over the calibration (1964-1973) and validation (1973-1984) periods.

years in both the calibration period (1962-1973) and validation period (1974–1983). A baseflow separation procedure was first conducted on the streamflow time series (Arnold and Allen, 1999; http://www.EnvSys.co.kr/~swatbflow), resulting in a ratio of baseflow to total flow ranging from 0.35 to 0.50 on an annual basis. Next, a sensitivity analysis was conducted with the SWATCUP SUFI2 software (Abbaspour, 2013), which involved running thousands of simulations and applying statistical tests to identify the parameters explaining greater variability in the model output. The most sensitive parameters were grouped according to the hydrologic flux that was most sensitive to the particular parameter, including runoff, baseflow, routing, and ET, and each grouping of parameters was varied one at a time. Performance metrics used in calibration and validation included the Nash-Sutcliffe Efficiency (NSE, Nash and Sutcliffe, 1970), coefficient of determination (R^2), and percent bias (Pbias) (Gupta et al., 1999). The ratio of simulated baseflow to total flow was required to be within the observed range ($0.35-0.50$), which resulted in slight adjustments after the initial calibration. Final adjusted parameter values for the hydrologic calibration are presented in Table S1 in the Supplementary Materials, in order of sensitivity. Full descriptions of each parameter are presented in the SWAT theoretical documentation (Neitsch et al., 2011).

Calibration of the plant growth model in SWAT followed a multi-step procedure based on comparing LAI, biomass, and fruit yield growth to field measurements, similar to the procedure in Heidari et al. (2019). The first step of the calibration process involved varying the sensitive LAI growth-related parameters, which include maximum potential LAI (BLAI) and the values of points that define the LAI-seasonal development and decline relationship (FRGRW1, FRGWRW2, LAIMX1, LAIMX2, and DLAI). Since it is recognized that SWAT typically does not simulate perennial vegetation growth in the tropics adequately (see for example, (Alemayehu et al., 2017), special attention was paid to adjusting the LAI-seasonal relationship parameters so that LAI did not exhibit dormancy at any time during the growth cycle. Second, biomass production, which comprises the total mass of the palms, was calibrated by changing the radiation use efficiency (Bio_E) and light extinction coefficient (EXT_coef) parameters. Third, harvest index parameters, which relate the fruit yield to biomass, were adjusted (HVSTI and HI_OVR). The LAI, biomass, and fruit yield growth models were calibrated with reported values from studies with different planting densities (Lamade and Setiyo, 1996; Corley and Tinker, 2008; Ishak and Awal, 2007; Gerritsma and Wessel, 1997; Goh, 1982). Higher ranges of reported values in the literature were used for matching fruit yield, since it was assumed that the palms are fully fertilized and water stress is unlikely due to high precipitation. The final adjusted parameter values for the vegetation growth model are presented in Table S2 in the Supplementary Materials. Full descriptions of these parameters are found in the SWAT theoretical documentation (Neitsch et al., 2011). Potential ET is calculated in SWAT with a Penman-Monteith model, requiring the hydroclimatic time series inputs described previously. Actual ET is dependent on canopy interception of precipitation, which in turn is controlled by LAI and maximum canopy storage values. Measured values of precipitation interception for oil plam (Chong et al., 2018; Farmanta and Dedi, 2015) were used calibrate the maximum canopy interception parameter (CANMX, see Table S2 in the Supplementary Materials for the range of calibrated values), following the procedure of Arnold (2012). Since the LAI models were calibrated for a range of planting densities, the actual ET varies with the particular planting density.

2.2. Modeling scenarios

The calibrated and validated model is used to simulate a range of oil palm conversion scenarios. In general, conversion to oil palm and subsequent fruit production are simulated as (a) initial planting of nursery stock in the first year of conversion; (b) a yield building phase, which lasts up to three years after planting (YAP) during which the canopy is not closed and no fruit is harvested; (c) a linear increase in fruits yield phase a (4–7 YAP); (d) a mature or plateau yield phase (8–14 YAP), (e) a yield decline phase (15–25 YAP), and (f) removal of the tree at 25 YAP (Woittiez et al., 2017; Fairhurst and Griffiths, 2014). Five planting densities were simulated (see Table 1) for each land use conversion scenario.

The most recent LULC map (2014, see land cover change analysis in Table S3 in the Supplementary Materials) is used to represent the Base Case scenario and assess the impacts of converting from existing t land cover types to oil palm. Analysis of land use change from 2000 to 2014 indicates that approximately 10 % of forest land was converted to agriculture and pasture during that period. Although the 2014 land cover map represents a period substantially later than the period of record for the hydroclimatic time series used in the calibration, the only parameter related to land cover that was adjusted during calibration was the curve number (CN). The calibrated CN values for each land use type and the other previously calibrated parameters are used for the new setup.

The impacts of allowing or disallowing conversion of existing cropland areas are simulated to assess policies of prohibiting land use competition between food crops and crops with potential industrial uses, such as using palm oil for biofuels. While current guidelines for optimal yield and minimizing soil erosion (Woittiez et al., 2017; Paramananthan, 2013) indicate that plantations occur

Table 1
Oil palm densities and associated maximum leaf area index (LAI) simulated in SWAT.

Density (palm/ha)	Maximum LAI
55	2.00
105	3.75
150	5.50
210	7.25
270	9.00

Table 2
Changes in the hydrologic fluxes as a result of oil palm conversion scenarios, relative to the Base Case scenario.

Scenario	Land Cover Converted to Oil Palm	Area (km^2)	Annual Precipitation (mm)	Base Case Annual ET (mm)	Base Case Annual Water Yield (mm)	Change in Annual ET from Base Case	Change in Annual Water Yield from Base Case
PF	Pasture	112.4	3780	836	2910	52 %	−15%
PF	Mixed Forest	7.8	4050	936	3080	37%	−11%
PF	Evergreen Forest	5.9	3360	813	2510	53 %	−17%
PF	Total/Mean	126.1	3777	841	2902	51 %	−15%
PFA	Pasture	112.4	3780	836	2910	52 %	−15%
PFA	Mixed Forest	7.8	4050	936	3080	37%	−11%
PFA	Evergreen Forest	5.9	3360	813	2510	53 %	−17%
PFA	Agriculture	88.5	3770	806	2940	50 %	−14%
PFA	Total/Mean	214.6	3774	827	2918	49 %	−14%
PFA +	Pasture	191.1	4048	882	3136	47%	−13%
PFA +	Mixed Forest	37.2	3930	869	3031	45%	−13%
PFA +	Evergreen Forest	7.1	4190	953	3209	36 %	−11%
PFA +	Deciduous Forest	4.4	4183	984	3172	36 %	−11%
PFA +	Agriculture	106	4128	932	3166	39 %	−11%
PFA +	Total/Mean	345.8	4064	899	3136	39 %	−11%

on lands with slopes less than 12 % (Corley and Tinker, 2008; Furumo and Aide, 2017), we also allow oil palm conversion on slopes as high as 30 %, to simulate the intensification of palm oil production due to higher demand and/or prices. The resulting four scenarios are then (a) Base Case; (b) conversion of pasture and forest (PF scenario) to oil palm on lands with slopes ≤ 12 % (127 km^2 converted, average elevation of converted land = 124 m above sea level, MASL); (c) conversion of crop, pasture and forest (PFA scenario) on lands with slopes ≤ 12 % (214 km^2 converted, average elevation of converted land = 132 MASL); and (d) conversion of crop, pasture and forest (PFA +) on lands with slopes ≤ 30 % (346 km^2 converted, average elevation of converted land = 219 MASL). Table 2 shows the areas of land use classes converted for each of the scenarios. Following a warm-up period to obtain initial conditions, each scenario simulation occurred over the 20-year period, using the 1964–1983 hydroclimatic time series.

The green water footprint is the volumetric water consumption associated with consumption of precipitation stored in the soil by a given production process that is otherwise available for evapotranspiration. The green water footprint is used as a metric to compare, for example, water to energy efficiency for biofuels and other energy sources (Hoekstra and Chapagain, 2006; Chiu and Wu, 2013). We report the green water use per mass of biomass and, by using literature values for the expected energy generated per unit of biomass, we convert the green water consumption per mass to green water consumption per unit of energy generated (Gerbens-Leenes et al., 2009). We then compare the green water footprints to literature values for oil palm fruit production and other biofuel feedstocks.

3. Results

3.1. Model performance evaluation

Comparison of simulated and observed monthly discharges is shown in Fig. 3. The Nash Sutcliffe efficiency of 0.72, R^2 of 0.74 and Pbias of 4.5 % for the entire simulation period indicates very good hydrologic model performance (Moriasi et al., 2007). Table S4 gives complete details of the model performance statistics for the calibration and verification periods. As shown in Fig. 4, comparison of the simulated versus measured oil palm yields demonstrates that the calibration of the plant growth model was reliable (R^2 = 0.81) over all phases of fruit production. Final adjusted parameter values for the hydrologic and vegetation growth model calibration are presented in Tables S1 and S2, respectively, in the Supplementary Materials. Area-weighted average values of the fitted curve

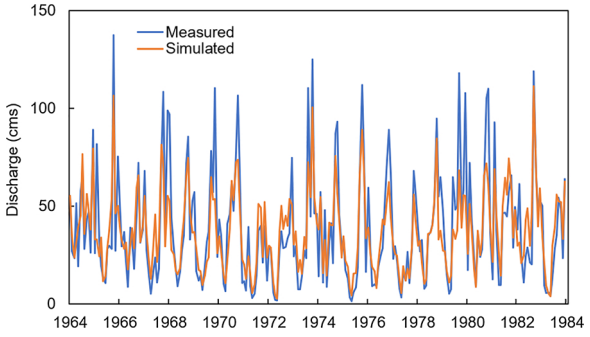

Fig. 3. Measured and modeled discharge during the calibration (1964-1973) and validation (1973-1984) periods.

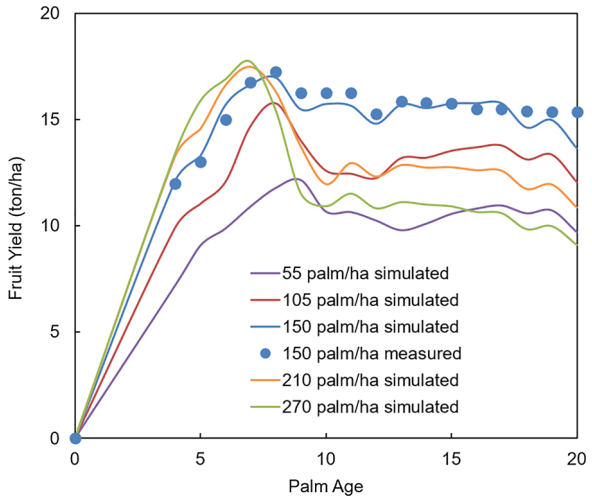

Fig. 4. Fruit yield simulation results versus time for different planting densities, with measured values for the 150 palm/ha planting density.

numbers for the land covers were as follows: oil palm CN = 75.4; agriculture CN = 88.6; pasture CN = 79.4; forest (averaged over mixed, evergreen, deciduous, and mixed forest) CN = 69.0.

3.2. Optimal planting density

Comparison across planting densities (Fig. 4) shows that the highest fruit production occurs with an average planting density of 150 palm/ha. At planting densities lower than 150 palm/ha, the yields are lower simply because there are fewer oil palms per cultivated area. While planting densities greater than 150 palm/ha are more productive in earlier years, competition for solar radiation causes a rapid decline in the yield starting in year 7 or 8 for the high planting densities. In the vegetation growth sub-model, fruit yield is a function of intercepted solar radiation and radiation use efficiency (RUE). RUE does not change with tree age, but light interception, LAI, and fruit yield increase with oil palm age. However, the fruit production simulations account for a decline in yield at a threshold around LAI of 6, as observed by Breure (2010), due to competition for solar radiation, resulting in the simulated declines in fruit production for higher planting densities. Fig. 5 shows the annual fruit yield versus the annual additional water use for all planting densities and scenarios. Additional water use is defined as the difference between ET for the base case and ET for a given conversion scenario for the converted land. These results indicate that, for every scenario, the 150 palm/ha planting density is the most efficient in terms of maximizing fruit production and minimizing additional water use. The increasing trend in efficiency from lower planting densities (55 and 105 palm/ha) to the 150 palm/ha planting density reflects a greater fractional increase in fruit production, due to the greater number of palms (see Fig. 4) than the corresponding fractional increase in water use. The smaller fractional increase in water use, compared to the increase in fruit production, is due to the lower sensitivity of ET to LAI, as compared

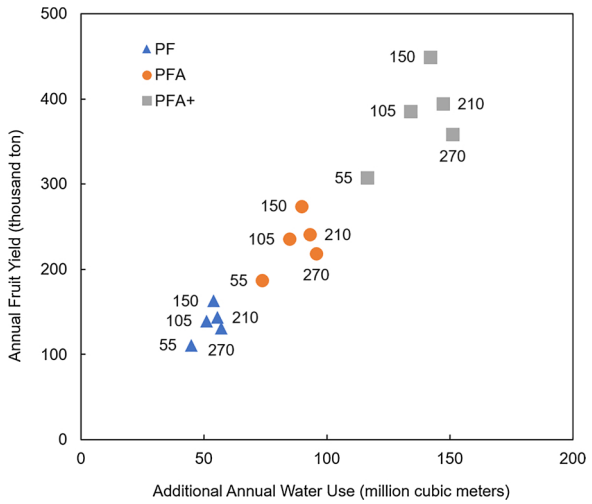

Fig. 5. Annual fruit yield versus additional water use for converted areas. Symbols indicate the respective conversion scenario. Numbers next to symbols indicate the respective planting density in palm/ha.

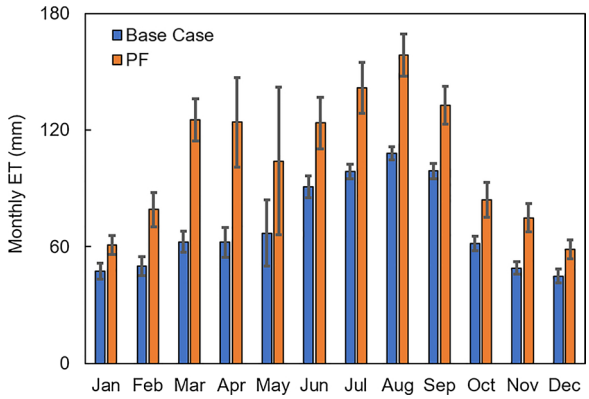

Fig. 6. Monthly mean ET rates for the PF scenario for the converted area for the Base case and PF scenarios. Error bars indicate one standard deviation of ET from the mean ET, with the standard deviation of ET calculated across the 20-year simulation period.

to the sensitivity of fruit production to LAI. The efficiency decreases when planting density increases from 150 palm/ha, indicating that fruit production decreases and water use increases. While the fruit yield declines steeply with planting density greater than 150 palm/ha (see Fig. 4), due to the threshold LAI that indicates radiative crowding, the increase in LAI with planting density tends to slightly increase the ET rate. Since the overall pattern of efficiency of water use per biomass production is similar across the planting densities (Fig. 5), results for only the most efficient density of 150 palm/ha are reported in the remaining text.

3.3. Hydrologic impacts in converted areas

Table 2 shows changes in average annual ET and yield for the land areas converted to oil palm for the three conversion scenarios, relative to the BAU scenario. These results show that the ET rate increases over a range of 36%–52% due to conversion to oil palm, with a corresponding decrease in water yield ranging from 11 % to 17 %. ET rates for the converted oil palm ranged from 1210 to 1340 mm/yr, with a mean of 1270 mm/yr. The higher ET rates for oil palm, compared to the prior land uses, are due to higher water use rates and higher LAI values. In general, higher changes in ET are found for conversion from the pasture and evergreen forest, since these land covers tended to have lower ET rates because of lower LAI and water use rates, respectively.

The results in Fig. 5 show that both the volumetric water use and fruit yield increase roughly linearly with the area of converted land for each scenario (PF: 127 km^2 converted; PFA: 214 km^2 converted; PFA+: 346 km^2 converted). The results in Table 2 also show that the increase in ET and subsequent decrease in water yield somewhat diminish from the PF to the PFA and PFA + scenarios. This trend can be explained by the mixture of land uses that are converted in each scenario. In the PFA scenario, the additional converted agricultural land produces a slightly smaller increase in ET compared to the other land conversions in the PF scenario, resulting in a small decrease in the change overall ET for the PFA scenario (49 %) compared to the PF scenario (51 %). However, for the PFA + scenario, the converted land classes have higher ET rates to begin with, because of the higher elevation in the watershed, which has the effect of reducing the increase overall ET rate substantially for the PFA + scenario (39 %) compared to the PFA scenario (49 %).

While the annual average increase in ET and decrease in water yield are substantial, the simulated monthly ET for the Base Case and the PF scenario, shown in Fig. 6, indicate that the seasonal impacts can be even greater. In March and April, ET increases by 100 % relative to the Base Case, due to higher temperatures and the palms reaching the yearly maximum LAI for these months. The error bars in Fig. 6 indicate the standard deviation of ET across the 20-year simulation period. The widths of the error bars for the PF conversion scenario are substantially greater, due both to the higher mean ET values and the higher sensitivity of ET rates to annual variations in climate for the PF oil palm conversion case than for the Base Case. In particular, the month of May displays an exceptionally high variability in ET across the 20 years. During the driest years (1971 and 1977, average precipitation of 2923 mm compared to annual precipitation of 3962 mm), the increase in ET and decrease in water yield were 60 % and 23 %, respectively, for the PF case compared to the Base Case. On average, the month of May has the greatest changes in water yield, with a reduction as large as 60 % in the driest year. Similar patterns of seasonal and inter-annual variations in ET were observed in the simulations of the PFA and PFA + scenarios (see Figure S2). Annual variations in the ET rate also depend, but to a lesser extent, on the life cycle of oil palm as the LAI increases and eventually reaches the maximum value in year 10 (see Figure S1).

Fig. 7 shows the average monthly decrease in water yield for the converted area for the PF scenario relative to the Base Case. The mean decreases are highest in May, due to lower rainfall and especially high temperatures (see Fig. 2), with decreases higher than 50 % in the driest years. Again, similar patterns of seasonal and inter-annual variations in water yield were observed in the PFA and PFA + scenario simulations (see Figure S3).

3.4. Watershed-scale impacts from land conversion scenarios

The model simulations indicate higher water use throughout the watershed as a result of oil palm conversions. Planting oil palm increases the ET rate over the whole watershed by 11 %, 18 % and 29 % for the PF, PFA and PFA + scenarios, respectively, compared

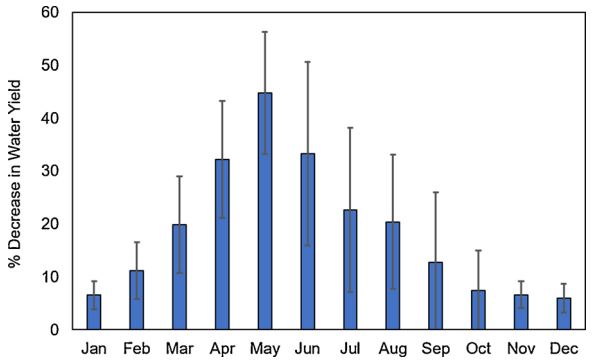

Fig. 7. Decrease in water yield from the converted area for the PF scenario relative to the Base case scenario. Error bars indicate one standard deviation of decrease in yield from the mean, with the standard deviation of decrease in yield calculated across the 20-year simulation period.

to the Base Case scenario. Due to the high annual precipitation rates in the watershed, especially in the southern portions of the watershed where the elevation increases above 2100 m ASL, the increases in ET only slightly affect the streamflow at the outlet, with 3%, 6% and 9% declines in average annual streamflows for the PF, PFA and PFA + scenarios, respectively. Interannual variation in climate produces a slightly larger decrease in the streamflow due to oil palm conversion in some years. During the driest years (1977 and 1971), annual streamflow at the outlet declines by 5.0 %, 8.6 % and 13.5 % under the PF, PFA and PFA + scenarios, respectively, relative to the Base Case scenario. In contrast, during the wet years (highest 25th percentile annual precipitation), streamflow at the outlet decreases by an average of 3%, 5% and 8% for the PF, PFA and PFA + scenarios, respectively. Fig. 8 shows the cumulative distribution functions (CDFs) of monthly watershed-scale streamflow for the Base Case, PF, PFA and PFA + scenarios over the simulation period. The CDFs for the PF, PFA and PFA + scenarios are almost identical in terms of the deviation from the Base Case scenario, except for the magnitude of low flows. For example, the 90 % exceedance flow for the PF and PFA + scenarios differ from the Base Case scenario by 16 % and 35 %, respectively.

At the sub-basin level, the simulation results indicate that sub-basin 1 (Fig. 1) will experience the greatest decline (24 %) in average annual water yield as a result of oil palm expansion for all three scenarios. On a seasonal basis, during the low-flow months of April, May and June, streamflow will decrease 50 % on average. The significant decline in annual and seasonal streamflows in sub-basin 1 is due to the low average annual precipitation in the sub-basin (2580 mm/year, which is 35 % lower than the watershed-wide average). For sub-basin 2, which has 50 % more rainfall than sub-basin 1 (3841 mm/year), the decline in average annual water yield in sub-basin 2 was only 14 %, although the fraction of converted land in sub-basin 2 was identical to that for sub-basin 1 for the PF scenario.

3.5. Green water footprint

The simulations indicate an ET water requirement of 0.98 to 1.4 m^3 to produce 1 kg of dry fruit, across the scenarios. This range is similar to the range of 1.1 to 1.4 m^3 water/kg fruit reported by Pleanjai et al. (2007) for oil palm cultivation in Malaysia. Assuming

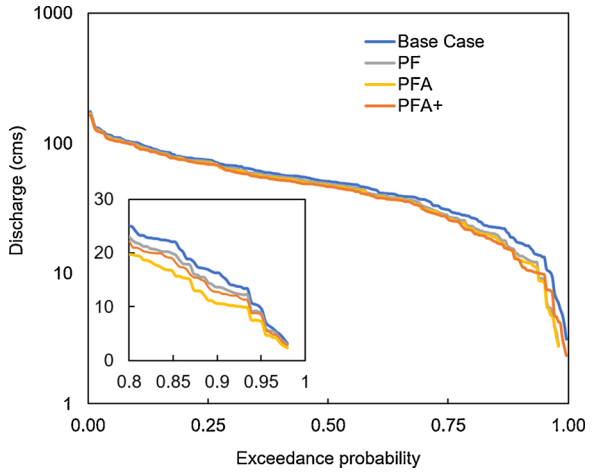

Fig. 8. Cumulative distribution functions (CDFs) of monthly streamflows at the watershed scale for the Base Case, PF, PFA and PFA + scenarios for the full simulation period (1964-1983). Inset shows the CDFs for the low flow tails of the CDFs.

each kilogram of fresh fruit (dry weight) can produce 0.30 kg of fuel (Pleanjai et al., 2007), the green water footprint is 3300 m^3 of water per 1 m^3 of biodiesel (biodiesel density = 874.7 kg/m^3, USDOE). Further assuming that the liquid fuel would have an energy content similar to conventional diesel fuels, 43 MJ/kg (International Gas Union, 2019), the green water footprint is 87 m^3 water/GJ. Babel et al. (2011) reports a slightly higher value of 110 m^3/GJ for biodiesel derived from oil palm in Thailand. If the green water footprint is calculated based on the additional ET relative to the Base Case scenario (shown in Table S6), the green water footprint is 0.34 m^3/kg of biomass or 25.2 m^3/GJ of energy.

In addition to conversion of the oil palm fruit, 50 − 70 tons/ha of biomass residue in the form of fiber, shell, palm kernel fronds, and trunks, can be collected over the life span of the oil palm (Salathong, 2007). The simulations conducted here indicate a total biomass production of 57 ton/ha (including fruit, above and below ground biomass), with 34 tons of biomass left as residue at the end of the 20-year simulation period. This residual is equivalent to an extra 323 GJ/ha, or a total of 4.0, 6.9 and 11.2 million GJ of bioethanol energy for the PF, PFA and PFA + scenarios, respectively, over the roughly 20-year lifetime of the oil palms.

4. Discussion

The ET rates for the converted oil palm ranged from 1210 to 1340 mm/yr for the 150 palm/ha planting density. These values of ET are on the lower end of values found in the literature, including Henson et al. (2007), Arshad (2014), Meijide et al. (2018), Tarigan et al. (2018) and Fan et al. (2019), who report mean ET rates from 1300 to 1800 mm/yr for sites in Indonesia and Malaysia. The lower ET for the Tabasco site, compared to the southeastern Asia sites, could be due to differences in climate, planting densities, and other hydrologic and vegetation conditions; however, one likely explanation is that the southeastern Asian sites are located close to the equator, compared to the mean latitude of 17.5° for the Tabasco site, which would lead to correspondingly lower solar radiation and ET in the Tabasco site.

The calibrated curve number for oil palm in this study was CN = 75.4 (areally averaged over all of the soil types), which is in the middle of the range of curve numbers found by Tarigan et al. (2016) for oil palm of CN = 67–89, with CN increasing as soils are less permeable. As Tarigan et al. (2016; 2018) have reported, conversion of forested land oil palm can lead to soil compaction. The curve number for oil palm found here is substantially higher than the average curve number for forest cover (69.0), which is an indirect indication that the soils were modified when converted for forest to land cover. In this work, however, other soil parameters, such as bulk density and available water content were constant for each soil type and were not adjusted based on land cover. The maximum LAI and calibrated maximum canopy interception ranged from BLAI = 2–9 and CANMX = 3–19, respectively, increasing as oil palm planting density increases. Tarigan et al. (2018) used values of BLAI = 3.6 and CANMX = 13.1 mm for a tree spacing of 8 m (approximately 140 palm/ha), which is roughly in the middle of planting densities used in this work. Tarigan et al.'s (2018) values of BLAI and CANMX fall roughly in the middle of the ranges found for these parameters in the present work.

Field and modeling studies from southeast Asia (e.g. Yusop et al., 2007; Adnan and Atkinson, 2011; van Griensven et al., 2014; Merten et al., 2016; Dislich et al., 2017; Tarigan et al., 2020) have demonstrated that conversion to oil palm plantations can substantially diminish streamflows. At the watershed scale and on an average annual basis, the results of this work imply that hydrologic impacts of oil palm conversion in this tropical Latin American region are minimal even for the scenario with the greatest area of conversion (PFA+). However, it is important to recognize that impacts at the watershed scale are subdued in this case because of the high overall precipitation rate in the watershed (~ 4000 mm/yr) and (b) the substantial fraction of land (~40 %) in the watershed that cannot be converted due to high slopes and elevations. On the other hand, the results found here demonstrate that substantial impacts on local-scale ET and water yield can occur at the scale of the converted lands, especially when seasonal and interannual variability are considered, corroborating the findings of van Griensven et al. (2014) and Tarigan et al. (2018).

The results also showed that impacts can be severe where precipitation rates are lower and where the converted land us has relatively low ET rates. For example, simulation results indicated that the highest relative increase in ET (53 %) and largest decrease in water yield (-17 %) occurred in lower precipitation areas (≤ 3200 mm/yr) where evergreen forest is converted. In the northern sub-basin, with 35 % less precipitation, simulations indicated a significant decline in the annual water yield (24 %) and a decrease in water yield of up to 50 % in the low-flow months of April to June. These results point to the potentially acute hydrologic impacts of oil palm plantations in areas with lower precipitation, such as other locations where oil palm is grown in the Americas, which have average annual precipitation between 1600 − 3500 mm/year (Woittiez et al., 2017). In areas with, for example, less than 3000 mm of rainfall, the increases in ET observed in the simulations presented here due to conversion to oil palm, streamflows at the watershed scale could be critically diminished, especially during dry seasons. We find that even for a wet region such as Tabasco, streamflows decreased by 35 % during the driest month for the case where approximately 60 % of the watershed was converted. Finally, areas where precipitation is expected to decline due to climate change may also be vulnerable to hydrologic impacts from palm oil conversion.

The results across the conversion scenarios indicate that the biomass production and the local hydrologic impacts, measured as loss in volumetric water yield, change linearly with the area of palm conversion, including the PFA + scenario. However, the PFA + scenario involves planting on steeply sloped lands, which could offer several disadvantages, including the potential for higher erosion rates and added labor or machinery expenses (Corley and Tinker, 2008). In addition, yields of oil palm have been known to decline on higher slopes because soils tend be shallower on higher slopes (Corley and Tinker, 2008). In the case of the study area, however, soil depths are relatively thick over all of the slopes in the PFA+, so shallow depths were not a factor in this case.

5. Conclusion

The main objective of this work was to study the hydrological impacts and water-biomass tradeoffs associated with the development of oil palm plantations for bioenergy production in a Latin American context. A SWAT model was used to simulate hydrologic fluxes and fruit production as a result of the conversion to a range of densities of oil palm from various land covers. The most efficient planting density in terms of water use and fruit production yield was 150 palm/ha. Hydrologic model simulations with this planting density indicated an 11 %–29 % increase in the overall ET rate of the watershed across the conversion scenarios. However, the higher water use did not result in a notable decline in the streamflow at the watershed scale, due to the high average annual precipitation in this region. Over the converted area, hydrologic model simulations indicated that the ET rates of oil palm were significantly higher (51 %) compared to the converted land covers, leading to a 15 % decline in average annual water yield and up to a 35 % decrease in monthly water yield from the converted area. At the sub-watershed scale, areas with lower precipitation had significant declines in the annual water yield (up to 24 %) and decreases in water yield of up to 50 % in the low-flow months of April to June.

Further hydrologic extensions of this work could consider impacts of conversion to oil palm on hydrologic properties such as soil compaction, which could result in higher runoff and consequently lower amounts of baseflow and diminished flows during low rainfall months. In addition, the potential negative impacts of oil palm conversion on water quality due to, for example, soil erosion and application of fertilizers could be simulated with a SWAT model. However, reliable water quality modeling will require careful, long term observations of parameters such as suspended solids and nutrients. Finally, since oil palm cultivation in low-lying lands with relatively low permeability soils typically requires drainage, in the impact of lowering the water table on seasonal flow needs to be investigated.

The local impacts of oil palm conversion on ET and water yields from various land covers identified in this study will help regional planners in determining the proportions of land covers that should be maintained to ensure effective water flow regulations at the watershed scale. In addition, the tradeoffs between biomass energy production and hydrologic impacts found here have important implications in determining which bioenergy crops are most suitable for a given hydroclimatic region. However, an integrated analysis of the potential impacts of oil palm conversion on the range of ecosystem service and socioeconomic outcomes is required to fully understand the sustainability of oil palm as a bioenergy feedstock.

CRediT authorship contribution statement

Azad Heidari: Conceptualization, Methodology, Writing - original draft. **Alex Mayer:** Supervision, Conceptualization, Writing - review & editing. **David Watkins:** Supervision, Conceptualization, Writing - review & editing. **María Mercedes Castillo:** Methodology, Writing - review & editing.

Declaration of Competing Interest

The authors report no declarations of interest.

Acknowledgments

We thank Cesar Jesús Vázquez Navarrete from the Colegio de Postgraduados, Campus Tabasco, for consulting on oil palm growth parameters for the study site. This material is based upon work supported by the National Science Foundation Research Coordination Network (RCN) Program (CBET #1140152).

Appendix A. Supplementary data

Supplementary material related to this article can be found, in the online version, at doi:https://doi.org/10.1016/j.ejrh.2020.100722.

References

Abbaspour, K.C., 2013. Swat-cup 2012. *SWAT Calibration and uncertainty program—A user manual*. EAWAG.
Adnan, N.A., Atkinson, P.M., 2011. Exploring the impact of climate and land use changes on streamflow trends in a monsoon catchment. Int. J. Climatol. 31 (6), 815–831.
Alemayehu, T., van Griensven, A., Woldegiorgis, B.T., Bauwens, W., 2017. An improved SWAT vegetation growth module and its evaluation for four tropical ecosystems. Hydrol. Earth Syst. Sci. 21 (9), 4449.
Arnold, J.G., Allen, P.M., 1999. Automated methods for estimating baseflow and ground water recharge from streamflow records 1. J. Am. Water Resour. Assoc. 35 (2), 411–424.
Arnold, J.G., Moriasi, D.N., Gassman, P.W., Abbaspour, K.C., White, M.J., Srinivasan, R., Santhi, C., Harmel, R.D., van Griensven, A., van Liew, M.W., Kannan, N., 2012. SWAT: Model use, calibration, and validation. Trans. ASABE 55 (4), 1491–1508.
Arshad, A.M., 2014. Crop evapotranspiration and crop water requirement for oil palm in peninsular Malaysia. J. Bio. Agric. Healthcare 4 (16), 23–28.
Babel, M.S., Shrestha, B., Perret, S.R., 2011. Hydrological impact of biofuel production: a case study of the Khlong Phlo Watershed in Thailand. Agric. Water Manag. 101 (1), 8–26.
Breure, C.J., 2010. Rate of leaf expansion: a criterion for identifying oil palm (*Elaeis guineensis* Jacq.) types suitable for planting at high densities. Wageningen J. Life Sci. 57 (2), 141–147.
Bruijnzeel, L.A., 2004. Hydrological functions of tropical forests: not seeing the soil for the trees? Agric. Ecosyst. Environ. 104 (1), 185–228.
Carlson, K.M., Curran, L.M., Ponette-González, A.G., Ratnasari, D., Lisnawati, N., Purwanto, Y., Brauman, K.A., Raymond, P.A., 2014. Influence of watershed-climate interactions on stream temperature, sediment yield, and metabolism along a land use intensity gradient in Indonesian Borneo. J. Geophys. Res. Biogeosci. 119 (6), 1110–1128.

Chiu, Y.W., Wu, M., 2013. The water footprint of biofuel produced from forest wood residue via a mixed alcohol gasification process. Environ. Res. Lett. 8 (3), 035015.
Chong, S.Y., Teh, C.B.S., Ainuddin, A.N., Philip, E., 2018. Simple net rainfall partitioning equations for nearly closed to fully closed canopy stands. Pertanika J. Trop. Agric. Sci. 41 (1).
Comte, I., Colin, F., Whalen, J.K., Grünberger, O., Caliman, J.P., 2012. Agricultural practices in oil palm plantations and their impact on hydrological changes, nutrient fluxes and water quality in Indonesia: a review. Advances in Agronomy Vol. 116. Academic Press, pp. 71–124.
Corley, R.H.V., Tinker, P.B., 2008. The Oil Palm. John Wiley & Sons.
Dislich, C., Keyel, A.C., Salecker, J., Kisel, Y., Meyer, K.M., Auliya, M., Barnes, A.D., Corre, M.D., Darras, K., Faust, H., Hess, B., 2017. A review of the ecosystem functions in oil palm plantations, using forests as a reference system. Biol. Rev. 92 (3), 1539–1569.
Fairhurst, T., Griffiths, W., 2014. Oil Palm: Best Management Practices for Yield Intensification. International Plant Nutrition Institute (IPNI), Singapore.
Fan, Y., Meijide, A., Lawrence, D.M., Roupsard, O., Carlson, K.M., Chen, H.Y., Röll, A., Niu, F., Knohl, A., 2019. Reconciling canopy interception parameterization and rainfall forcing frequency in the Community Land Model for simulating evapotranspiration of rainforests and oil palm plantations in Indonesia. J. Adv. Model. Earth Syst. 11 (3), 732–751.
FAOSTAT, 2017. Online Statistical Service. FAOSTAT. http://www.fao.org/faostat/en/#data/QC.
Farmanta, Y., Dedi, S., 2015. Rainfall interception by palm plant canopy. In: International Seminar on Promoting Local Resources for Food and Health, 12-13 October. Bengkulu, Indonesia.
Fuka, D.R., Walter, M.T., MacAlister, C., Degaetano, A.T., Steenhuis, T.S., Easton, Z.M., 2014. Using the Climate Forecast System Reanalysis as weather input data for watershed models. Hydrol. Process. 28 (22), 5613–5623.
Furumo, P.R., Aide, T.M., 2017. Characterizing commercial oil palm expansion in Latin America: land use change and trade. Environ. Res. Lett. 12 (2), 024008.
Gerbens-Leenes, W., Hoekstra, A.Y., van der Meer, T.H., 2009. The water footprint of bioenergy. Proc. Natl. Acad. Sci. 106 (25), 10219–10223.
Gerritsma, W., Wessel, M., 1997. Oil palm: domestication achieved? Wageningen J. Life Sci. 45 (4), 463–475.
Gilroy, J.J., Prescott, G.W., Cardenas, J.S., Castañeda, P.G.D.P., Sánchez, A., Rojas-Murcia, L.E., Medina Uribe, C.A., Haugaasen, T., Edwards, D.P., 2015. Minimizing the biodiversity impact of Neotropical oil palm development. Glob. Change Biol. 21 (4), 1531–1540.
Goh, K.H., 1982. Analyses of oil palm spacing experiments [Malaysia]. In: In International Conference on Oil Palm in Agriculture in the Eighties. Kuala Lumpur (Malaysia), 17-20 Jun 1981. PPP (ISP).
Gupta, H.V., Sorooshian, S., Yapo, P.O., 1999. Status of automatic calibration for hydrologic models: comparison with multilevel expert calibration. J. Hydrol. Eng. 4 (2), 135–143.
Hardanto, A., Röll, A., Niu, F., Meijide, A., Hölscher, D., 2017. Oil palm and rubber tree water use patterns: effects of topography and flooding. Front. Plant Sci. 8, 452.
Heidari, A., Mayer, A., Watkins, D., 2019. Hydrologic impacts and trade-offs associated with forest-based bioenergy development practices in a snow-dominated watershed, Wisconsin, USA. J. Hydrol.
Henson, I.E., Yahya, Z., Noor, M.R.M., Harun, M.H., Mohammed, A.T., 2007. Predicting soil water status, evapotranspiration, growth and yield of young oil palm in a seasonally dry region of Malaysia. J. Oil Palm Res. 19, 398–415.
Hoekstra, A.Y., Chapagain, A.K., 2006. Water footprints of nations: water use by people as a function of their consumption pattern. Integrated Assessment of Water Resources and Global Change. Springer, Dordrecht, pp. 35–48.
Instituto Nacional de Estadística y Geografía- INEGI, http://www.inegi.org.mx/.
International Gas Union, 2019. NIST Chemistry WebBook, OECD/IEA Electricity Information (various editions), Natural Gas Conversion Guide. (Accessed on march 2019). http://www.world-nuclear.org/information-library/facts-and-figures/heat-values-of-various-fuels.aspx.
Ishak, W., Awal, M.A., 2007. Leaf area index model for oil palm FFB yield prediction. Pertanika J. Trop. Agric. Sci. 30, 51–56.
Lamade, E., Setiyo, I.E., et al., 1996. Test of Dufrêne's production model on two contrasting families of oil palm in North Sumatra. In: Ariffin, D. (Ed.), Proceedings of the 1996 PORIM International Palm Oil Congress Competitiveness for the 21st Century. Palm Oil Research Institute of Malaysia, Kuala Lumpur. pp. 427–435.
Larsen, R.K., Jiwan, N., Rompas, A., Jenito, J., Osbeck, M., Tarigan, A., 2014. Towards 'hybrid accountability in EU biofuels policy? Community grievances and competing water claims in the Central Kalimantan oil palm sector. Geoforum 54, 295–305.
Ludwig, F., Biemans, H., Jacobs, C., Supit, I., van Diepen, C.A., Fawell, J., Capri, E., Steduto, P., 2011. Water Use of Oil Crops: Current Water Use and Future Outlooks. ILSI Europe aisbl.
Manoli, G., Meijide, A., Huth, N., Knohl, A., Kosugi, Y., Burlando, P., Ghazoul, J., Fatichi, S., 2018. Ecohydrological changes after tropical forest conversion to oil palm. Environ. Res. Lett. 13 (6), 064035.
Meijide, A., Badu, C.S., Moyano, F., Tiralla, N., Gunawan, D., Knohl, A., 2018. Impact of forest conversion to oil palm and rubber plantations on microclimate and the role of the 2015 ENSO event. Agric. For. Meteorol. 252, 208–219.
Merten, J., Röll, A., Guillaume, T., Meijide, A., Tarigan, S., Agusta, H., Dislich, C., Dittrich, C., Faust, H., Gunawan, D., Hein, J., 2016. Water scarcity and oil palm expansion: social views and environmental processes. Ecol. Soc. 21 (2).
Moriasi, D.N., Arnold, J.G., Van Liew, M.W., Bingner, R.L., Harmel, R.D., Veith, T.L., 2007. Model evaluation guidelines for systematic quantification of accuracy in watershed simulations. Trans. Asabe 50 (3), 885–900.
Mukherjee, I., Sovacool, B.K., 2014. Palm oil-based biofuels and sustainability in southeast Asia: a review of Indonesia, Malaysia, and Thailand. Renewable Sustainable Energy Rev. 37, 1–12.
Nash, J.E., Sutcliffe, J.V., 1970. River flow forecasting through conceptual models part I—a discussion of principles. J. Hydrol. 10 (3), 282–290.
Neitsch, S.L., Arnold, J.G., Kiniry, J.R., Williams, J.R., 2011. Soil and Water Assessment Tool Theoretical Documentation Version 2009. Texas Water Resources Institute.
Paramananthan, S., 2013. Managing marginal soils for sustainable growth of oil palms in the tropics. J. Oil Palm Environ. Health (JOPEH) 4.
Pirker, J., Mosnier, A., Kraxner, F., Havlík, P., Obersteiner, M., 2016. What are the limits to oil palm expansion? Glob. Environ. Change 40, 73–81.
Pleanjai, S., Gheewala, S.H., Garivait, S., 2007. Environmental evaluation of biodiesel production from palm oil in a life cycle perspective. Asian J. Energy Environ. 8 (1–2), 15–32.
Ramankutty, N., Graesser, J., 2017. Latin American oil palm follows an unfamiliar route to avoid deforestation. Environ. Res. Lett. 12 (4), 041001.
Röll, A., Niu, F., Meijide, A., Hardanto, A., Knohl, A., Hölscher, D., 2015. Transpiration in an oil palm landscape: effects of palm age. Biogeosciences 12 (19), 5619–5633.
Salathong, J., 2007. The Sustainable Use of Oil Palm Biomass in Malaysia with Thailand's Comparative Perspective. See also: http://www.wiaps.waseda.ac.jp/initiative/2006/intern/group_02/PDF/Jessada% 20Salathong.pdf. .
Sheil, D., Casson, A., Meijaard, E., Van Noordwijk, M., Gaskell, J., Sunderland-Groves, J., Wertz, K., Kanninen, M., 2009. The Impacts and Opportunities of Oil Palm in Southeast Asia: What Do We Know and What Do We Need to Know? Vol. 51 Center for International Forestry Research, Bogor, Indonesia.
Sumarga, E., Hein, L., Hooijer, A., Vernimmen, R., 2016. Hydrological and economic effects of oil palm cultivation in Indonesian peatlands. Ecol. Soc. 21 (2), 52. https://doi.org/10.5751/ES-08490-210252.
Tarigan, S.D., Wiegand, K., Dislich, C., Slamet, B., Heinonen, J., Meyer, K., 2016. Mitigation options for improving the ecosystem function of water flow regulation in a watershed with rapid expansion of oil palm plantations. Sustainability Water Qual. Ecol. 8, 4–13.
Tarigan, S., Wiegand, K., Slamet, B., 2018. Minimum forest cover required for sustainable water flow regulation of a watershed: A case study in Jambi Province, Indonesia. Hydrol. Earth Syst. Sci. 22 (1), 581–594.
Tarigan, S., Stiegler, C., Wiegand, K., Knohl, A., Murtilaksono, K., 2020. Relative contribution of evapotranspiration and soil compaction to the fluctuation of catchment discharge: case study from a plantation landscape. Hydrol. Sci. J. Des Sci. Hydrol. 65 (7), 1–10.
van Griensven, A., Maharjan, S., Alemayehu, T., 2014. mproved simulation of evapotranspiration for land use and climate change impact analysis at catchment scale. Proceedings-7th International Congress on Environmental Modelling and Software: Bold Visions for Environmental Modeling, iEMSs 2014 2, 979–986.
Vijay, V., Pimm, S.L., Jenkins, C.N., Smith, S.J., 2016. The impacts of oil palm on recent deforestation and biodiversity loss. PLoS One 11 (7), e0159668.
Winchell, M., Srinivasan, R., Di Luzio, M., Arnold, J., 2013. ArcSWAT Interface for SWAT2012: User's Guide. Blackland Research and Extension Center, Texas Agrilife Research. Grassland. Soil and Water Research Laboratory, USDA Agricultural Research Service, Texas, pp. 3.
Woittiez, L.S., van Wijk, M.T., Slingerland, M., van Noordwijk, M., Giller, K.E., 2017. Yield gaps in oil palm: a quantitative review of contributing factors. Eur. J. Agron. 83, 57–77.
Yusop, Z., Chan, C.H., Katimon, A., 2007. Runoff characteristics and application of HEC-HMS for modelling stormflow hydrograph in an oil palm catchment. Water Sci. Technol. 56 (8), 41–48.